How important is sample alignment in planar biaxial testing of anisotropic soft biological tissues? A finite element study

Heleen Fehervary, Julie Vastmans, Jos Vander Sloten, Nele Famaey

Biomechanics Section, KU Leuven, Leuven, Belgium

Abstract

Finite element models of biomedical applications increasingly use anisotropic hyperelastic material formulations. Appropriate material parameters are essential for a reliable outcome of these simulations, which is why planar biaxial testing of soft biological tissues is gaining importance. However, much is still to be learned regarding the ideal methodology for performing this type of test and the subsequent parameter fitting procedure.

This paper focuses on the effect of an unknown sample orientation or a mistake in the sample orientation in a planar biaxial test using rakes. To this end, finite element simulations were conducted with various degrees of misalignment. Variations to the test method and subsequent fitting procedures are compared and evaluated.

For a perfectly aligned sample and for a slightly misaligned sample, the parameters of the Gasser-Ogden-Holzapfel model can be found to a reasonable accuracy using a planar biaxial test with rakes and a parameter fitting procedure that takes into account the boundary conditions. However, after a certain threshold of misalignment, reliable parameters can no longer be found. The level of this threshold seems to be material dependent.

For a sample with unknown sample orientation, material parameters could theoretically be obtained by increasing the degrees of freedom along which test

*Corresponding author: H. Fehervary, KU Leuven, Biomechanics Section, Celestijnenlaan 300C, 3001 Heverlee (Belgium)

data is obtained, e.g. by adding the data of a rail shear test. However, in the situation and the material model studied here, the inhomogeneous boundary conditions of the test set-ups render it impossible to obtain the correct parameters, even when using the parameter fitting method that takes into account boundary conditions.

To conclude, it is always important to carefully track the sample orientation during harvesting and preparation and to minimize the misalignment during mounting. For transversely isotropic samples with an unknown orientation, we advise against parameter fitting based on a planar biaxial test, even when combined with a rail shear test.

Keywords: constitutive modeling, planar biaxial testing, rakes, rail shear testing, parameter fitting, FE simulations, unknown sample orientation

---

1. Introduction

Finite element (FE) modeling of biomedical applications has considerable potential to improve medical treatment. For example, the use of *in silico* clinical trials can reduce the need for expensive animal and *in vivo* clinical trials, and FE modeling enables patient-specific planning of surgical treatment. The material description of the soft tissues in FE models is crucial to accurately predict deformations and stresses when loads are applied to a certain geometry. Mechanical material characterization of soft biological tissues is therefore an active research domain.

Soft biological tissues are heterogeneous and exhibit non-linear, anisotropic and visco-elastic mechanical behavior. To characterize this behavior, different set-ups for *in vitro* mechanical testing are available, applying different types of loading along one or multiple axes: uniaxially (tensile, indentation, rail shear), biaxially (planar tensile, extension-inflation) and triaxially (extension-inflation-torsion, biaxial tensile-shear).

While the community performing mechanical tests on soft biological tissues is growing, standardized protocols are lacking and the effects of certain assump-

tions have only partially been investigated. Especially for planar biaxial testing, the effect of different gripping mechanisms, i.e. rakes, sutures or clamps, is significant but not well understood. The effect of the gripping mechanism or other testing conditions can be studied using FE modeling. Sun *et al.* compared clamps to sutures for planar biaxial testing [**?**]. Other groups have focused on changing conditions (e.g. loading protocol) for a planar biaxial test using rakes [**?** **?**] or changing sample shape for a planar biaxial test using clamps [**?**] or sutures [**?**]. Nolan and McGarry investigated the shear forces present in planar biaxial tests with clamps, caused by the confined transversal movement at the clamps [**?**].

While most of the aforementioned papers consider the homogeneity of the stress-strain field at the center of a sample as a quality measure of the performed mechanical test, we believe that the quality of the resulting material parameter estimation is equally if not more important if the results are subsequently used in a FE simulation. Our previous work investigated the effect of several loading conditions and provided guidelines for planar biaxial testing with rakes [**?**]. This paper continues to study planar biaxial tensile testing with rakes, now focusing on the effect of an unknown orientation of the test sample with respect to the tissue's material axes.

Biological soft tissue's anisotropic behavior can usually be attributed to the presence of collagen fiber families along a preferential direction. Often, two or more collagen fiber families are oriented symmetrically with respect to a natural axis of the tissue, e.g. the circumferential direction in case of arteries [**?**]. As a consequence, the orientation of test samples with respect to the native geometry is an important variable and should be tracked. For example, when a cylindrical segment of arterial tissue is harvested and prepared for planar biaxial testing, a square sample is excised such that the circumferential and axial direction can be aligned with the test axes of the set-up. However, quite often the orientation of the sample can not be recovered or is unclear, e.g. when the sample is resected from an irregular or incomplete segment of tissue. Furthermore, imperfections during mounting might also lead to a misalignment between the test axes and

the tissue's symmetry axes.

A consequence of an unknown or incorrect orientation of a test sample is that the collagen fibers will most likely not be oriented symmetrically with respect to the test axes. In a planar biaxial set-up, this results in shear deformations and stresses, although shear deformation is often assumed negligible in planar biaxial testing [**? ? ?**]. The goal of this paper is to investigate the effect of a rotated sample orientation in a planar biaxial test using rakes on the resulting material parameter estimation. To this end, we simulate a number of virtual planar biaxial tests using FE modeling, with various material parameter sets and varying sample rotations. Subsequently, we perform material parameter fitting on the virtual test results to see if we can retrieve the imposed material parameters. We also investigate how the addition of a rail shear experiment can improve the results.

The outline of this paper is as follows: first the different test variations and their FE model are described. Next, details are given on the strain calculation, the sample material model, the parameter fitting and accompanying quality measures. The next section shows the results, including the deformations and forces of the different tests and the fitted parameters. Finally, these results are discussed and a conclusion is formulated.

2. Materials and Methods

This section first describes the general principles of the two test types that are considered: a planar biaxial test using rakes and a rail shear test, since we investigate whether addition of the latter can improve overall parameter fitting results. Next, a FE model of both test types is constructed and a series of FE simulations with different material parameters and sample orientations is conducted. The material model used is the Gasser-Ogden-Holzapfel material [**?**] and the strain in both tests is measured using markers. For all simulations a parameter fitting is conducted. Different combinations of tests and parameter fitting procedures are used. Finally, quality measures for parameter fitting

results are described.

2.1. Test types

Two different test types for thin and planar samples are considered: a planar biaxial test using rakes and a rail shear test (see Figure **??**). In both tests, square-shaped samples are used where often markers or speckles are applied in the central area of the sample. Hence, the deformation of the sample can be extracted from continuous camera image acquisition during the test. This allows the tracking of sample deformation without influence of tear or slippage at the clamping site. The description that follows is to ensure a good understanding of the boundary conditions of the tests, which will be reproduced numerically as described in Section **??** and of the numerical simulation.

2.1.1. Planar Biaxial test with Rakes (PBR)

In a rake-based planar biaxial test, rakes are used to mount the four sides of a square, planar sample. Rakes are stiff needles that are pierced through the tissue. The holes created by mounting are further referred to as sample holes. During the test a normal force or displacement is applied simultaneously on the four sets of rakes. The data acquired in this type of test is the evolution through time of the normal force at the rake sets (i.e. not for each individual rake) and the displacement field of the markers or speckles (see Section **??**).

2.1.2. Rail shear test (RS)

In a rail shear test, two sides of a sample are mounted using clamps, resulting in a rectangular testing area, with its long edge parallel to the clamped edge. One clamp is then displaced tangential to the clamped edge, while the normal distance between the clamps is fixed. This approximates a simple shear deformation. The data acquired during this test are the images of the deformed sample and the shear traction force and, in case of a multi-axial load cell, the normal force.

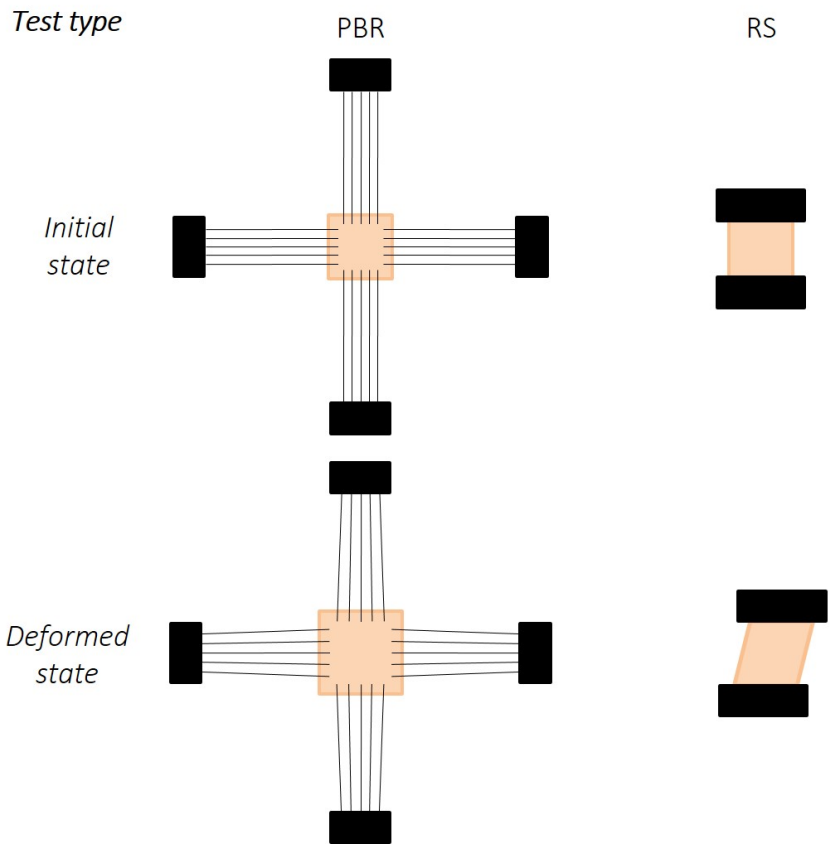

Figure 1: An overview of the test types considered: a planar biaxial test using rakes (PBR) and a rail shear (RS) test. Each test is shown in initial and deformed state. Adapted from [**?**].

2.2. Finite element simulation

This section gives details on the FE modeling of the tests described in Section **??**. Using the FE software Abaqus 6.14-1 (Dassault Systmes Simulia Corp., Providence Rhode Island, USA), the sample is modeled in the 12-plane with the thickness or radial direction in the 3-direction. If the orientation of the sample is known, the circumferential and axial direction are aligned with the 1- and 2-direction, respectively.

The samples are modeled with M3D4R elements. Membrane elements are surface elements that transmit in-plane forces and have no bending stiffness [**?**

]. For each test a mesh convergence analysis was performed. As a convergence criterion the error of the force ratio between a mesh with n elements and a mesh with $2n$ elements was monitored [**?**]. The force ratio was calculated as the experimental traction force over the model traction force (see Section **??**). The number of elements was increased until the convergence error was $\leq$ 2%. The simulations were performed in Abaqus Standard and the maximum increment of the time step was limited, such that at least 30 data points were available when exporting data from the simulation. The data corresponding to what would be available in a real experiment (typically forces and markers coordinates) are exported from the simulation.

2.2.1. Planar Biaxial test with Rakes (PBR)

A sketch of the FE model of the PBR test is shown in Figure **??**. The sample is 7 mm by 7 mm with different thickness values, the latter depending on the simulated sample (see Section **??**). The mesh consists of 32 331 elements. Each side of the sample has five sample holes through which the rakes are pierced. Four nodes located in the center of the sample and forming a square are used as markers. The dimensions of the sample can be seen in Figure **??**.

The rakes are modeled based on BioRakes (CellScale, Waterloo, Canada). A rake has a length of 30 mm and consists of 8 B33 elements. These beam elements can be used to model slender beams, where the cross-section is small compared to the axial length [**?**]. The cross section or profile of the beam is modeled as a circle with radius 0.15 mm. The material of the rakes is linear elastic with properties of stainless steel: a Young's modulus of 195 GPa and a Poisson ratio of 0.31. Each rake is connected to the sample by kinematic coupling: the semi-circle of the sample hole follows the normal displacements of the rake tip, and one point on the semi-circle also follows the transversal displacement of the rake tip. In this way the sample hole is allowed to enlarge, which can also happen during a real experiment.

To obtain a strain level of approximately 30% in the central area of the sample, a nominal displacement of 0.88 mm is applied at the distal node of each

of the rakes, in the direction normal to the undeformed sample edge. Different ratios for the first and second direction are used for the displacement: (1-1) (0.5-1) and (1-0.5). All other degrees of freedom of the distal nodes of the rakes are fixed as well as the central node of the sample. An overview of the mesh and the boundary conditions is shown in Figure **??**. The reaction forces at the end of the rakes and the coordinates of the markers are exported for each time step.

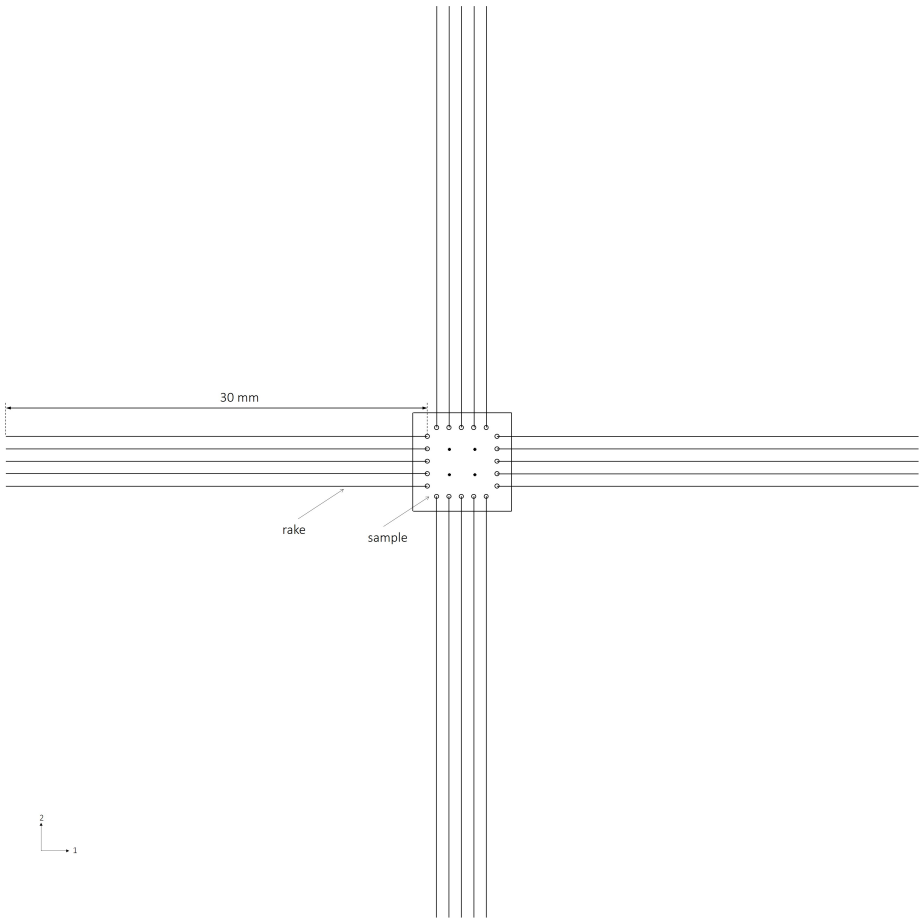

Figure 2: Sketch of the FE model of the planar biaxial test using rakes (PBR). The model consists of a sample and 20 rakes.

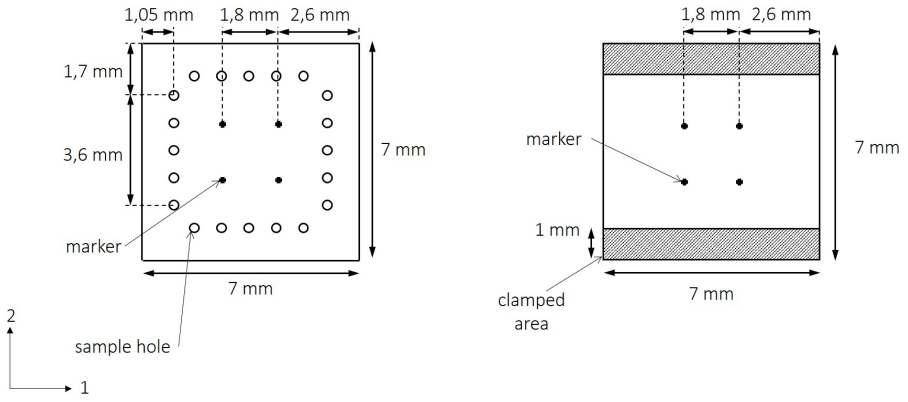

Figure 3: The sample dimensions of both test types (PBR and RS). The markers are located in the central area of the sample.

2.2.2. Rail shear test (RS)

Figure **??** shows a sketch of the FE model of the RS test and its dimensions. The sample is 7 mm by 7 mm and again has various thickness values (see Section **??**). The mesh consists of 4720 elements. The markers are modeled as four nodes located in the central area of the sample in a rectangular shape. A section of 1 mm high at the bottom end of the sample is clamped, meaning that all degrees of freedom of these nodes are fixed. At the top end of the sample again a section of 1 mm high is clamped, where all degrees of freedom are fixed, except for the transversal 1-direction, which is displaced by a distance of 3.5 mm in both senses consecutively. The reaction forces at the top surface and the coordinates of the markers are exported for each time step.

2.3. Strain calculation: deformation gradient

During these type of experiments, the strain in the 12-plane is typically measured using a camera in combination with markers or speckles that are attached to the sample. In this study, markers are used. The in-plane components of the

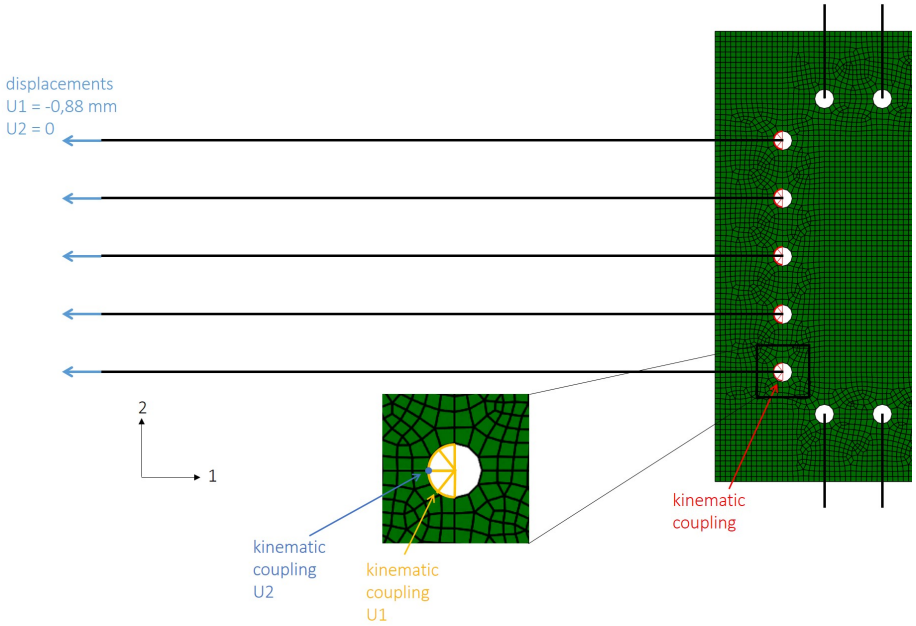

Figure 4: In the FE model of PBR the sample and the rakes are connected via kinematic coupling between the semi-circle of the sample hole and the rake tip. The outer end of the rakes are displaced in the normal direction.

deformation gradient

$$\boldsymbol{F} = \begin{bmatrix} F_{11} & F_{12} & 0 \\ F_{21} & F_{22} & 0 \\ 0 & 0 & F_{33} \end{bmatrix} \tag{1}$$

can be calculated by the method of Hoffman and Grigg [**?**]. In this method, the four markers are considered to build up a two dimensional element. Assuming incompressibility of the biological tissue, volume preservation (or $J = \det(\boldsymbol{F}) = 1$) allows the calculation of $\boldsymbol{F}_{33}$ as

$$F_{33} = \frac{1}{F_{11}F_{22} - F_{12}F_{21}}. \tag{2}$$

2.4. Material

2.4.1. Material model

The material of the sample is described using the Gasser-Ogden-Holzapfel model (GOH) [**?**] which defines a strain energy density function (SEDF) Ψ as

$$\Psi = C_{10}(I_1 - 3) + \sum_{i=4,6} \frac{k_1}{2k_2} \left[e^{k_2(\kappa I_1 + (1-3\kappa)I_i - 1)^2} - 1 \right]. \tag{3}$$

The SEDF is a combination of a linear isotropic term, representing the contribution of the matrix material and an exponential anisotropic term, representing the contribution of collagen fibers. I_1 is the first invariant of the right Cauchy-Green strain tensor $\boldsymbol{C} = \boldsymbol{F}^T\boldsymbol{F}$. I_4 and I_6 are two pseudo-invariants of $\boldsymbol{C}$ related to the stretch in the direction of the two fiber families.

$$I_1 = tr(\boldsymbol{C}) \tag{4}$$

$$I_{4,6} = \boldsymbol{M_i} \cdot (\boldsymbol{C}\,\boldsymbol{M_i}), \tag{5}$$

where $\boldsymbol{M_i}$ is the fiber vector of the fiber family i in the undeformed configuration. It expresses the mean direction of the fibers using the fiber angle α_i, defined with respect to the circumferential direction,

$$\boldsymbol{M_i} = \begin{bmatrix} \cos(\alpha_i) \\ \sin(\alpha_i) \\ 0 \end{bmatrix}. \tag{6}$$

C_{10} [MPa] and k_1 [MPa] represent the stiffness of the matrix material and collagen fibers, respectively. k_2 [-] is related to the non-linearity of the collagen fibers. κ [-] reflects the dispersion of the fibers and has a value between 0 (no dispersion) and 1/3 (full dispersion).

For arterial tissue, the assumption of symmetric fiber families with respect to the circumferential direction is often made [**?**]. When the orientation of the sample is known, the circumferential direction is aligned with a test axis. The relation between both fiber angles is known in this case: $\alpha_2 = -\alpha_1$, and

Table 1: The ground truth material parameter sets for the GOH model.

NAME	C_{10} [MPa]	k_1 [MPa]	k_2 [-]	κ [-]	α_1 [RAD]	α_2 [RAD]	thickness [mm]
MM1-0	0.0770	0.0078	18.5600	0.2060	0.4800	2.6616	2.65
MM1-8	0.0770	0.0078	18.5600	0.2060	0.6196	2.8013	2.65
MM1-20	0.0770	0.0078	18.5600	0.2060	0.8290	3.0107	2.65
MM1-45	0.0770	0.0078	18.5600	0.2060	1.2654	0.3054	2.65
MM2-0	0.0872	0.0063	3.3500	0.0000	0.2601	2.8815	2.95
MM2-8	0.0872	0.0063	3.3500	0.0000	0.3997	3.0212	2.95
MM2-20	0.0872	0.0063	3.3500	0.0000	0.6091	0.0890	2.95
MM2-45	0.0872	0.0063	3.3500	0.0000	1.0455	0.5253	2.95

only one material parameter α is required for material modeling. When the orientation of the tissue is unknown, this relation is unknown, and hence two material parameters α_1 and α_2 are required to describe the material model. Thus 5 or 6 material parameters are to be determined to model a material that is symmetric or asymmetric with respect to the test axes, respectively.

2.4.2. Ground truth material parameter sets

The material parameters used as ground truth values in the FE simulations are two sets that describe thoracic aorta aneurysmal tissue [**?**]. The orientation of the samples is changed from symmetric with respect to the test axes, slightly rotated (over 8°), more rotated (over 20°) to maximally asymmetric (rotated over 45°). With these different orientations, the influence of a small mistake in orientation or of an unknown orientation can be estimated. The sets are shown in Table **??** with the corresponding sample thickness.

2.4.3. Model stresses and traction forces

The first Piola-Kirchhoff stress $\boldsymbol{P}$ is calculated as the derivative of the SEDF with respect to the deformation gradient [**?**] as

$$\boldsymbol{P}^{mod} = -p\boldsymbol{F}^{-T} + \frac{\partial \Psi}{\partial \boldsymbol{F}}, \tag{7}$$

where the scalar p is introduced for incompressible materials and serves as an indeterminate Lagrange multiplier. It can be considered a hydrostatic pressure and is determined from boundary conditions. In the case of planar tensile experiments (such as PBR and RS), p can be determined from the planar stress state, since

$$\sigma_{33}^{mod} = 0. \tag{8}$$

The Cauchy stress $\boldsymbol{\sigma}$ is calculated from the first Piola-Kirchhoff stress $\boldsymbol{P}$ as

$$\boldsymbol{\sigma} = J^{-1}\boldsymbol{P}\boldsymbol{F}^T, \tag{9}$$

with $J = \det(\boldsymbol{F})$ the Jacobian determinant or volume ratio of the deformation gradient.

The first Piola-Kirchhoff stress is related to the traction force $\boldsymbol{t}$ as [**?**]

$$t_{ij} = P_{ij}A_j. \tag{10}$$

Here, t_{ij} is the force in the i-th direction applied on a surface with the normal in the j-th direction. Note that for equation **??** there is no summation over j, i.e. Einstein notation is not used. Note also that in other engineering disciplines, a different convention might be used.

2.5. Parameter fitting

A material model, e.g. the one described in Section **??**, describes a tissue's behavior using material parameters. The latter are calibrated to match the experimental data as well as possible using a parameter fitting procedure. This section first gives details on the objective of this optimization problem, its different components and its weights and then describes the different parameter fitting procedures.

2.5.1. Components of the objective function

Parameter fitting is solving an optimization problem or minimizing a certain objective function, that might be subjected to constraints. The objective function of the parameter fitting used here, compares traction force data measured experimentally to the corresponding traction force data computed using the material model.

Each of the test set-ups described in Section **??** has different boundary conditions, yielding differences in the corresponding objective function. In what follows, the components of the objective function are described for both test types: PBR and RS.

PBR.

In a PBR test, the displacements and forces are measured along the two test axes. In most set-ups only the normal force is measured of the entire set of rakes. The objective function therefore compares the following components of the traction force data: $n = 11, 22$.

RS.

In a RS test, the shear force and displacement of the top surface along the 1-direction are measured. According to our convention for traction force (see Section **??**), the component of the traction force in the objective function of this test type is: $n = 12$.

2.5.2. Combining different set-ups: weights

When different experiments are conducted on multiple samples of the same tissue, this data can be combined in one parameter fitting and hence one objective function. In this case, weights should be used to assign adequate importance to each data set. Three different types of weights can be distinguished.

The first weight type $w^s_{n,1}$ corrects for the number of data points of each set. The data sets with a lower number of data points, receive a higher weight such that each test has an equal contribution to the objective. Hence, the weight for a specific set is the ratio between the maximum number of data points of all

sets over the number of data points of that specific set.

The second weight type $w^s_{n,2}$ corrects for the range of traction force. Usually, with an increasing traction force, the difference between model and experimental traction force in the objective function also increases. This weight assures an equal contribution between different tests with different force ranges. It is calculated as the lowest maximum traction force of all objective components over the maximum traction force of that objective component. In other words, this weight scales the traction forces to the lowest maximum traction force of all samples and sets.

The third weight type $w^s_{n,3}$ is assigned by the user. The user can for example decide to assign a higher weight to a test depending on its reliability. In this case the user weights were all 1.

The total weight for a component of the objective function relating to an objective component n of a sample s is then

$$w_{s,n} = w^s_{n,1} w^s_{n,2} w^s_{n,3}. \tag{11}$$

2.5.3. Objective function

The objective function O of the parameter fitting problem is a combination of the components n for every sample s and their weights $w_{s,n}$. For every component, the difference between the experimental and model traction force vector $\boldsymbol{t}$ is minimized,

$$O = \sum_s \sum_n (w_{s,n}(\boldsymbol{t}^{mod}_n - \boldsymbol{t}^{exp}_n))^2. \tag{12}$$

2.5.4. Parameter boundaries and constraints

The boundaries of the parameters are shown in Table **??**. Note that the upper boundaries of C_{10}, k_1 and k_2 are not based on a physical quantity or limit but are chosen far enough removed from typically observed values. The lower boundaries of C_{10} and k_2 are not exactly 0 to avoid numerical issues in the FE simulations.

Table 2: The boundaries for the material parameters of the GOH model.

NAME	C_{10} [MPa]	k_1 [MPa]	k_2 [-]	κ [-]	α_i [RAD]
lower boundaries	1e-4	0	1e-4	0	0
upper boundaries	1	10	100	1/3	π

In the case of five fitting parameters, the objective function is not subjected to any constraint. In the case of six fitting parameters, a constraint is applied to assure that both fiber angles α_i do not end up in the same value. In this case the objective function is subjected to

$$\alpha_2 > \alpha_1 + 10^\circ \frac{\pi}{180^\circ}. \tag{13}$$

2.5.5. Procedure

Different procedures for parameter fitting exist: the classic parameter fitting, inverse FE parameter fitting and the parameter fitting that corrects for the inhomogeneities caused by the boundary conditions in the experimental set-up. This study uses the first and last procedure, discussed below.

Classic parameter fitting.
In the optimization process of a classic parameter fitting, the material parameters are altered until the objective function is minimized. In that case the model traction forces are as close as possible to the experimental traction forces. The optimization problem can be solved analytically, since the model traction forces are a closed form of the input variable, i.e. the deformation gradient. In our implementation, the optimization problem was solved in Matlab 2015b (The Mathworks Inc., Natick, Massachusetts, USA) with the CasAdi toolbox [**?**] using Optistack [**?**]. 10 different initial starting points were used to assure a global minimum was found.

Boundary Conditions Corrected (BCC) .
The Boundary Conditions Corrected (BCC) parameter fitting procedure was

previously developed by the authors [**?**] [1] and takes into account the effects of the boundary conditions that lead to an inhomogeneous stress-strain field and corrects for the simplifications that are made in the data processing. For example: in a planar biaxial experiment with rakes, the forces and displacements are applied at five discrete points. However, in the data processing, it is assumed that the force is applied in a continuous manner. As shown in [**?**], this assumption leads to incorrect material parameters. The scheme of the BCC method is shown in Figure **??**. First, a classic parameter fitting is conducted on the experimental data obtained from a mechanical experiment. The resulting parameters are then used to perform a FE simulation of this mechanical experiment. A correction vector $\boldsymbol{g}$ is calculated component-wise as the ratio between the model and experimental traction forces from the FE simulation. This correction vector $\boldsymbol{g}$ is then used in the objective function of the BCC parameter fitting to compensate for the assumptions made in the classic parameter fitting. This loop can be repeated until a stop criterion is reached.

2.6. Quality measures for goodness of fit

In general, the goodness of fit reflects the answer to the following question: how well does the model reflect the experimental data? To this end a Normalized Root Mean Square Error (NRMSE) can be calculated between the experimental and model data. Actually, this is the square root of the mean value of the objective function O,

$$\mathrm{NRMSE}_O = \sqrt{\frac{\sum_s \sum_n w_{s,n} \sum_i (t_{n,i}^{mod} - g_{n,i} t_{n,i}^{exp})^2}{m}}, \tag{14}$$

with s the number of samples, n the objective components and i the entries of the vector $\boldsymbol{t}$. m is the total number of entries for all objective components and all samples: $m = s \cdot n \cdot i$. $g_{n,i}$ is the value of the correction vector for the objective component n at time i. This value is 1 in case of a classic parameter

[1] Note that the method was previously, i.e. in [**?**], referred to as Inhomogeneity from Experimental set-up Corrected (IEC)

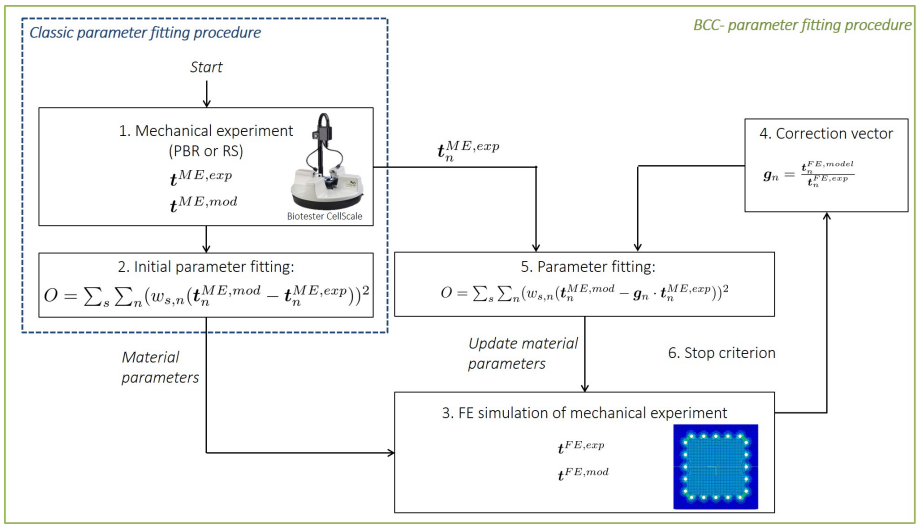

Figure 5: Overview of the BCC parameter fitting procedure. A FE simulation is conducted to correct for the assumptions made in the classic parameter fitting. Adapted from [**?**].

fitting. It is considered normalized, as the weights $w_{s,n}$ contain a division by the maximum traction force (see Section **??**). Note that we do not use the Pearson correlation coefficient or coefficient of determination, as these coefficients are meant for linear models and the GOH model considered here is non-linear.

In this case, as we work with virtual experiments, we know the ground truth material and can therefore also consider another question: how correct is the result of the parameter fitting compared to the ground truth? To answer this question, two quality measures are used: a Mean Percentage Error (MPE_{GT}) and a NRMSE_{GT}. The resulting fitted parameters themselves can be compared to the ground truth parameters using a MPE_{GT}. The MPE_{GT} is calculated as

$$\text{MPE}_{GT} = \frac{1}{p} \sum_i \frac{|FP_i - GP_i|}{|GP_i|}, \tag{15}$$

with FP_i the fitted parameter i, GP_i the ground truth parameter i and p the number of fitted parameters. The MPE thus reflects how correct the parameters are compared to the ground truth parameters.

The NRMSE_{GT} is used to compare the difference between the model traction

forces calculated with the ground truth parameters and the fitted parameters,

$$\mathrm{NRMSE}_{GT} = \sqrt{\frac{1}{m}\sum_{s}\sum_{n}\frac{\sum_i (t_{n,i}^{mod}(FP) - t_{n,i}^{mod}(GP))^2}{\max(\boldsymbol{t}_n^{mod}(GP))}}, \tag{16}$$

with s, n, i and m as mentioned before. $\boldsymbol{t}^{mod}(FP)$ and $\boldsymbol{t}^{mod}(GP)$ are calculated based on the fitted and ground truth parameters, respectively. The NRMSE_{GT} thus reflects how well the fitted traction forces approximate the ground truth traction forces, regardless of the values of the parameters.

A final measure to assess the quality of the fitted parameters is to extrapolate them to a different loading domain and compare the results to the ground truth. To this end, the Cauchy stress σ is calculated, as explained in Section **??**, for a deformation gradient corresponding to a uniaxial tensile test. This is done using the ground truth as well as the fitted material parameters.

3. Results

This section shows the results in different subsections: first, the deformations and forces of both test types are shown. Secondly, the difference between the experimental and the ground truth model traction forces is visualized and finally, the results of the different parameter fittings are presented.

3.1. Deformation and force

This subsection shows the normal and shear forces as a function of the deformation for the different sets of FE simulations of both test types. The deformation is calculated from the displacement of the markers for each test type. The forces are those that in a physical experiment would be measured with a multi-axial load cell. Note however, that often only one-axis load cells are available in actual experimental set-ups. The forces and deformations are shown for both material sets in every orientation.

3.1.1. PBR test

The forces and deformations of a MM1 and MM2 sample mounted with different orientations in a PBR test using a 1-1 loading ratio are shown in Figures **??** and **??**, respectively. The forces and deformations in the normal directions are much larger than those in the shear directions. When the sample is not mounted symmetrically with respect to the test axes of a PBR (MM1-8, MM1-20, MM1-45, MM2-8, MM2-20 and MM2-45), the shear deformations and forces increase with respect to the symmetric mounting case (MM1-0 and MM2-0), but are still orders of magnitude smaller than the normal deformations and traction forces. The non-symmetric mounting also influences the behavior in the normal directions. While the non-linear behavior is still visible in the 11-direction for MM2-8, it is less pronounced for MM2-20 and no longer visible for MM2-45. The magnitude of the shear deformations and forces depends on the material parameters and on the orientations of the fibers. For MM1-45 and MM2-45 the behavior seems isotropic: the curves are the same in the 11- and 22-direction and in the 12- and 21-direction. The deformed states of all samples with varying orientations tested in a PBR are shown in Figure **??**. The deformed state does not show a lot of difference between the different sample orientations.

3.1.2. RS

Figures **??** and **??** show the forces and deformations of a MM1 and MM2 sample, respectively, tested in a RS with different orientations. The left and right hand plots correspond to a displacement of the top surface of 3.5 mm and -3.5 mm, respectively. The shear traction force is higher than the normal traction force, but can be in the same order of magnitude, depending on the sample material. The deformation in the normal direction is limited. When the sample orientation is rotated, the force-stretch curves change. The deformed state of all samples is shown in Figure **??**. For different sample orientations, the deformed states look the same.

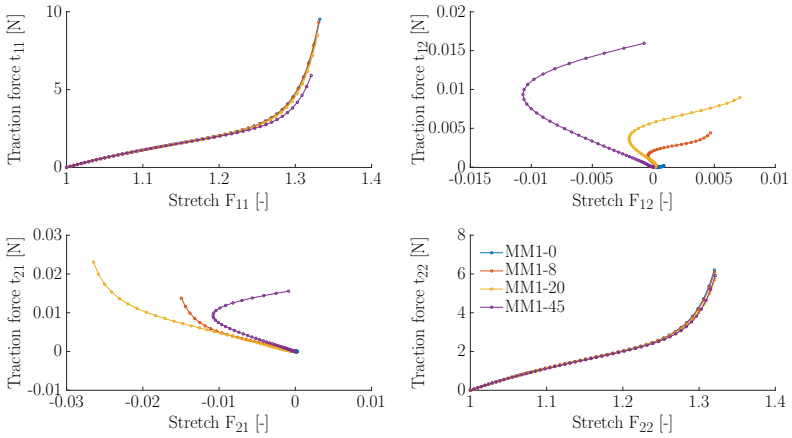

Figure 6: Forces as a function of deformation for a sample with MM1 material. The sample orientation is varied from mounted symmetrically to maximally asymmetrically with respect to test axes in a PBR test. The forces and deformations in the normal directions are much larger than those in the shear directions. Note that the four plots should be interpreted together given the multi-axial loading situation.

3.2. Experimental and ground truth model traction forces

Figures **??** and **??** show the experimental traction forces as measured during the experiment and the ground truth model traction forces, calculated from the ground truth material parameters and the deformation measured during the experiment. The forces are shown for MM1-0 and MM2-0 for a 1-1 loading ratio in the case of PBR test, and a 3.5 mm top surface displacement in the case of RS test. The difference between the experimental and ground truth model traction forces is caused by the boundary conditions of the set-up and by assumptions made in the data processing [**?**]. Due to this difference, the ground truth material parameters can never be found using a classic parameter fitting procedure. The BCC parameter fitting procedure compensates for this difference, in order to approximate the ground truth.

3.3. Parameter fitting

This subsection shows the results of the different cases for which parameter fitting was performed. More specifically, the classic (C) procedure and two

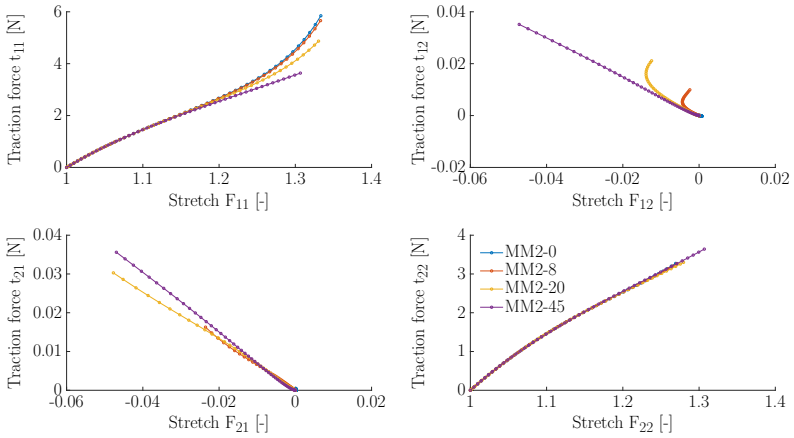

Figure 7: Forces as a function of deformation for a sample with MM2 material. The sample orientation is varied from mounted symmetrically to maximally asymmetrically with respect to test axes in a PBR. The forces and deformations in the normal directions are much larger than those in the shear directions. Note that the four plots should be interpreted together given the multi-axial loading situation.

iterations of the BCC procedure, were performed. In the first case, the sample orientation is assumed to be known, i.e. the sample material is assumed to be mounted symmetrically with respect to the test axes. Hence five material parameters of the GOH model need to be calibrated. In this first case, the sample is tested on a PBR (5-PBR). In the second and third case, the sample orientation is assumed to be unknown, which means that the sample is no longer assumed to be mounted symmetrically with respect to the test axes and six material parameters need to be calibrated. In the second case, the sample is tested on a PBR (6-PBR) and in the third case, a combination of a PBR and a RS test is used (6-PBR+RS). Note that for all cases of PBR tests, the three loading ratios were used for the parameter fitting. The tables with the results from the material parameter fitting and the quality measures are shown in the Appendix.

An overview figure of the above cases is shown in Figure **??**. It visualizes the quality measures from Tables **??**, **??** and **??** used to asses how well the result

Figure 8: Deformed state of the different sample orientations tested in a PBR. It is not possible to estimate from the deformed state in a PBR whether the test axes and material axes are aligned.

of the parameter fitting approximates the ground truth.

Comparing the classic and the BCC parameter fitting results, the MPE_{GT} is lower for the BCC parameter fitting in most of the cases and the NRMSE_{GT} is always lower for the BCC parameter fitting. This means that the approximation of the ground truth material parameters is mostly better and the approximation of the ground truth model traction forces is always better when BCC parameter fitting is used.

When the sample orientation is known (MM1-0 & MM2-0) or when there is only a small deviation in the sample orientation (MM1-8 & MM2-8), the performance of the three different fitting cases is similar. When the sample orientation is unknown (MM1-20, MM2-20, MM1-45 & MM2-45), the performance of 6-PBR+RS is better than the other cases.

Figure **??** shows the stress-strain curves of the extrapolation of the parameter fitting results to a uniaxial tensile test. The parameters obtained via the Classic and the BCC parameter fitting from the three cases mentioned before are used and compared to the ground truth. It can be observed that the stress-strain curves calculated from the material parameters obtained via the BCC procedure are a better approximation of the ground truth than those calculated from the material parameters obtained via the Classic procedure. The stress-strain curves of MM1-45 and MM2-45 do not approximate the ground truth for any of the three cases.

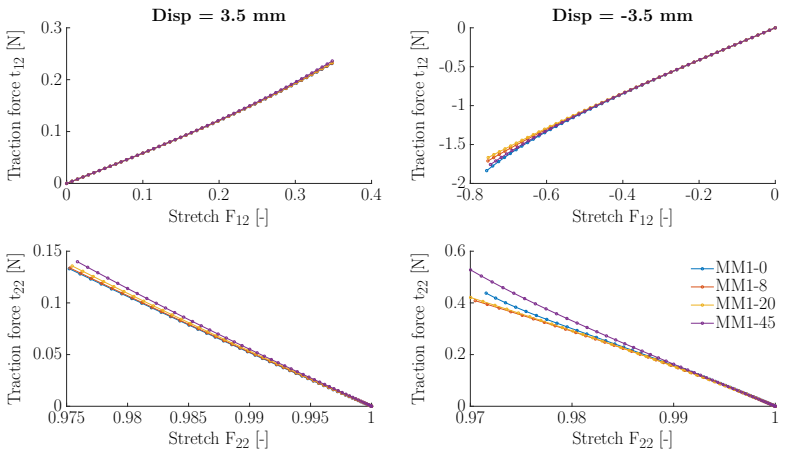

Figure 9: Forces as a function of deformation for a MM1 sample with varying orientation tested using RS. The applied displacement on the top surface is 3.5 mm (left hand side) and -3.5 mm (right hand side). With a changing orientation, the force-stretch curves change. Note that the top and bottom curves pertain to the same test and should be interpreted together.

4. Discussion

The aim of this study was first to investigate the consequences of a rotated sample orientation in a PBR and RS test (i.e. when the material axes are no longer aligned with the test axes), and second, to examine material parameter fitting results when the sample orientation is unknown or deviated. This section discusses the obtained results and is divided in different subsections. First, the effects of a rotated sample orientation on the obtained test data are discussed, next different aspects of the effects on parameter fitting results are treated: BCC parameter fitting, a mistake in sample orientation and an unknown sample orientation. Finally, a general discussion is held.

4.1. Effect of sample orientation on the obtained test data

To investigate the effect of a rotated sample orientation, a FE simulation of a PBR and a RS test was conducted with different sample materials and different sample orientations. Deformations and forces were exported from these simulations as if they were real tests with a multi-axial load cell.

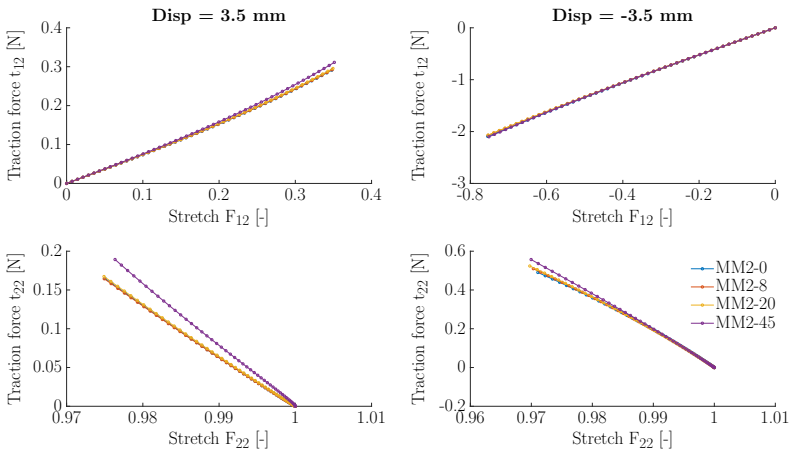

Figure 10: Forces as a function of deformation for a MM2 sample with varying orientation tested using RS. The applied displacement on the top surface is 3.5 mm (left hand side) and -3.5 mm (right hand side). With a changing orientation, the force-stretch curves change. Note that the top and bottom curves pertain to the same test and should be interpreted together.

Figure 11: Deformed state of the different sample orientations tested in a RS. It is not possible to estimate whether the test axes and material axes are aligned from the deformed state.

In a PBR test, shear deformation and forces are orders of magnitude smaller than the normal ones (see Figures **??** & **??**). When the sample orientation is varied, shear deformations and forces increase, but are still small with respect to the normal ones. This can be expected, as the boundary conditions of a PBR test (i.e. the stiff rakes), restrict shear deformation (see Figure **??**). The assumption made in different studies that shear can be neglected in a PBR test (e.g. [**?**], is therefore valid. It is worth to note that a planar biaxial test using sutures on a pulley system on the other hand, does allow shear deformation. It is therefore important to understand the different types of planar biaxial tests

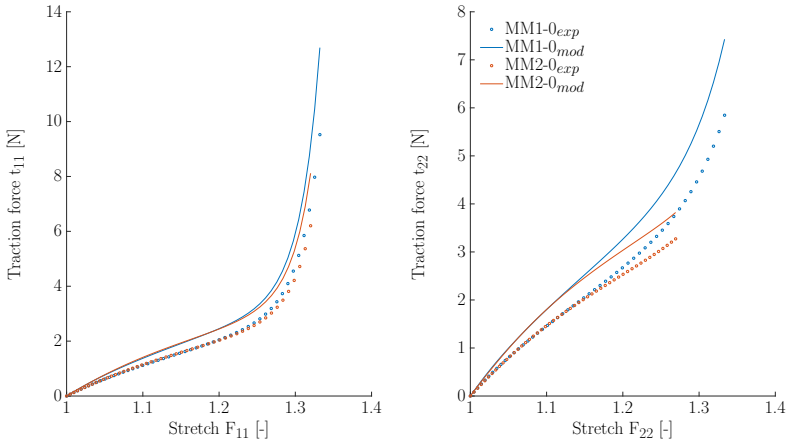

Figure 12: Experimental and ground truth model traction forces from a MM1-0 and MM2-0 sample tested in a PBR. The difference between experimental and ground truth model is caused by the boundary conditions of the set-up and assumptions made during the data processing.

(using rakes, clamps or sutures), since the different gripping mechanisms lead to different boundary conditions and hence, different deformations and forces. Results of these different types of planar biaxial tests, can therefore not be compared without taking these differences into account.

In a RS test, the shear force can be in the same range as the normal force and the normal deformation is limited. When the sample orientation is varied, the force-stretch curves change.

In both test types, the obtained test data change as the sample orientation varies. The sample can appear either more stiff or more compliant when rotated. The amount of change depends not only on the amount of rotation, but also on the sample material. When the test data changes, this will be reflected in the parameter fitting. It is therefore important to carefully track the sample orientation during harvesting and test preparation. When the sample orientation is unknown, or when the material symmetry is disrupted because of disease, other, preferably non-destructive, methods (histology, microscopy, μCT) can be used to provide information on the number of fiber families and their orientation.

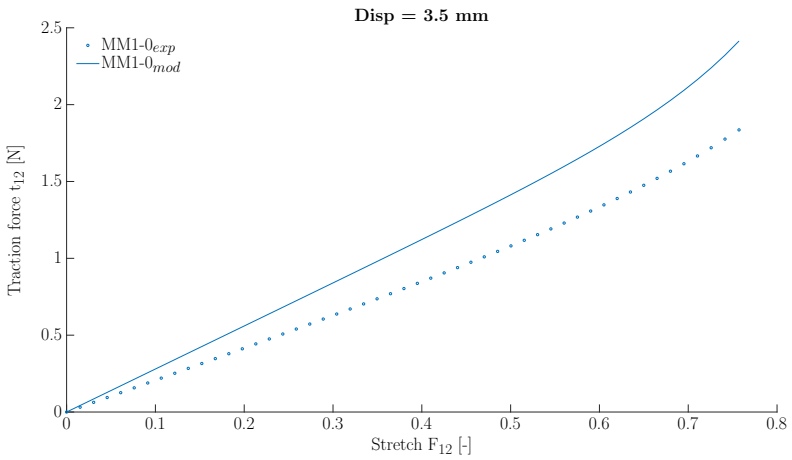

Figure 13: Experimental and ground truth model traction forces from a MM1-0 and MM2-0 sample tested in a RS. The difference between experimental and ground truth model is caused by the boundary conditions of the set-up and assumptions made during the data processing.

Destructive methods or methods that influence the material behavior should be avoided if not enough sample material is available.

4.2. Effect of BCC parameter fitting

As shown in Figures **??** & **??**, there is a difference between the experimental traction forces and the ground truth model traction forces. As the experimental traction forces are used for parameter fitting, the ground truth parameters will never be found when this difference is not compensated for. This difference is related to the boundary conditions of the test and the assumptions made in the data processing. The BCC parameter fitting procedure estimates this difference using a FE simulation and compensates for it [**?**]. This is reflected in the parameter fitting results: the MPE$_{GT}$ and NRMSE$_{GT}$ in general decrease when using BCC parameter fitting. Also, when the resulting material parameters are extrapolated, the ones obtained with the BCC procedure are a better approximation of the ground truth (see Figure **??**).

Convergence of the BCC procedure has been reached when the NRMSE$_{GT}$ no longer decreases for increasing BCC iterations. In some cases the results after

the second BCC iteration are a less good approximation of the ground truth parameters than after the first BCC iteration. Moreover, it can be noticed that the convergence is slower in some cases than in others. Note that in reality the NRMSE_{GT} can not be calculated, as the ground truth is unknown. This shows the importance of a good stop criterion for the BCC parameter fitting procedure, which is subject of future research.

It can be seen for example for MM1-0 & MM2-0 in Table **??** that the results of the classic parameter fitting are indeed a poor estimation of the ground truth parameters. Using the BCC procedure, the approximation of the ground truth improves: decreasing MPE_{GT} and NRSME_{GT}. Sometimes the MPE_{GT} increases with increasing BCC iterations. However, if the NRMSE_{GT} decreases, a better approximation of the ground truth traction forces is still obtained. The increase of MPE_{GT} can be explained by the convexity of the objective function. If the objective function is locally flat, different sets of material parameters will result in a similar value of the objective function. Of course, when the objective function changes, e.g. when evaluating a different loading condition, the objective function can change as well and the plateau might disappear. Therefore, the local shape of the objective function should be investigated to asses the quality of the parameter fitting results. In general, care is needed when parameters are extrapolated to a loading range different to the one they were calibrated on.

4.3. Effect of a mistake in the sample orientation

When the material axes of the sample are not aligned with the test axes of a set-up, but it is assumed that they are aligned, this is considered as a mistake in the sample orientation. In this case, the measured forces and deformations change and shear deformations and forces increase (see Figures **??** & **??**).

A small mistake in orientation causes only a small deviation of the force-stretch curves with respect to the sample that is not rotated. This is also reflected in the parameter fitting results (see Table **??**). With a mistake of 8°, the NRMSE_{GT} of MMx-0 and MMx-8 are similar after the classic procedure

and bigger than after the BCC procedure. This can also be observed in Figure **??** where the stress-strain curves calculated with the material parameters obtained with the BCC procedure are a better approximation of the ground truth compared to those obtained with the Classic procedure. Hence, using the BCC parameter fitting to correct for the difference between the model and experimental forces is more important than avoiding a small mistake in sample orientation.

With an increasing mistake in sample orientation, the deviation of the force-stretch curves increases. Also the mistake in parameter fitting results increases accordingly, up to a point at which even the BCC procedure can no longer correct for it. The estimation of the parameters related to the non-linearity and the fibers (k_1, k_2, κ and α) is poor. The amount of deviation of the force-stretch curves for a certain mistake in sample orientation depends on the sample material, making it difficult to set a fixed angle above which fitting results cannot be trusted. Moreover, a mistake in sample orientation is hard to detect from the deformed sample tested in a PBR (see Figure **??**).

When the sample is rotated over 45° (MM1-45 & MM2-45), the behavior of the sample appears to be isotropic. This is reflected in the parameter fitting with κ going to 1/3. Hence, α no longer has a meaning. The value of α is no longer optimized and this is reflected with very high MPE_{GT} values. When these material parametes are extrapolated to uniaxial loading, the resulting stress-strain curves are far from the ground truth (see Figure **??**).

However, note that when such a sample would be tested in a planar biaxial test using sutures, this mistake in orientation would be easier to detect. This type of test allows shear deformation, which occurs when the test axes are not aligned with the material axes. Nevertheless, the latter test type brings other drawbacks, especially regarding difficulties in mounting, making it perhaps also more prone to sample orientation errors than a PBR test.

4.4. Effect of unknown sample orientation

When the sample orientation is unknown, an extra fitting parameter needs to be calibrated. From Table **??**, it can be seen that the data from a PBR test is not always enough to calibrate the six parameters. This is in accordance with the theory [**?** **?**]. While for a known sample orientation, the SEDF depends on two independent invariants, $\Psi(I_1, I_4)$, for an unknown sample orientation, the SEDF depends on three independent invariants: $\Psi(I_1, I_4, I_6)$. However, from a PBR test, only two independent components of deformation and traction forces are available (F_{11} and F_{22}, and t_{11} and t_{22}, respectively). Therefore, it is theoretically possible to characterize a sample with known orientation, but impossible to characterize a sample with unknown orientation.

The combination of a PBR with a RS test results in a third independent component of deformation and traction force (F_{12} and t_{12}). Hence, in theory it should be enough to characterize a sample with unknown orientation. This is true for the case of an ideal PBR test and an ideal RS test, i.e. with perfectly homogeneous deformation fields (results not shown). However, as shown in Table **??**, for a PBR and a RS test with realistic boundary conditions, the ground truth parameters are only found in some cases using the BCC parameter fitting procedure. It is possible that by a further addition of test data (e.g. adding a uniaxial test or even more ratios), the parameter fitting results would improve further.

While, according to theory, the material parameters should be found by combining PBR and RS test, and the BCC method is used to compensate for the fact that realistic set-ups are used instead of ideal ones, the correct parameters can not always be found. A possible cause can be that the BCC method has slow convergence if the first parameter estimation is far from the ground truth. Another possible cause is related to the shape of the objective function as explained before. Increasing the amount of information in the objective function, e.g. by adding an extra loading condition, can be a solution for this.

The addition of the RS test leads to a decrease in MPE_{GT}, however the MPE_{GT} of MM2-0 and MM2-8 are an exception. Hence, though counter-

intuitive, increasing the amount of test data, does not always result in an improved parameter fitting result.

Another consideration is the fact that the addition of the RS test will cause a change in the weights of the objective function $w_{s,n}$. In this case the weights for the PBR test will decrease. The NRMSE_{GT} is calculated without weights, and thus the addition of a RS test might cause an increase in the overall NRMES_{GT}. Perhaps a better balance between the two tests, different from the weights that are used now, could improve the outcome. This balance is likely to be dependent on the sample material, which is why the effect of weights in an objective function should be studied further in the future. Also the effect of constraints (e.g. equation **??**) on the result of the parameter fitting should be further investigated. For example, now a difference between the fiber angles of 10° was enforced and the optimization did not seem sensitive to small changes, but this might again dependent on the sample material and on the shape of the objective function.

4.5. General discussion

This paper investigates the influence of a sample's orientation on the test data and parameter fitting of a PBR and a RS test and helps to increase the understanding of the a set-up and its boundary conditions. A similar analysis could be made for other set-ups. The FE models of the PBR and RS test used in this study contains realistic boundary conditions. In a real experiment though, even more inaccuracies (such as rakes positions, noise on the load cell) will be present. Moreover, a RS test is sensitive to wrinkling for higher levels of shear strains. A preload along the normal axis can help reduce this wrinkling. These inaccuracies and undesired effects will influence the test data and should be accounted for as much as possible.

Another assumption made here is the fact that two samples are available with exactly the same material properties: one for a PBR test and another one for a RS test. In reality, variations in material behavior can exist within one harvested biological tissue. This assumption can be overcome, if it would be

possible to perform both test types on the same set-up.

In addition, the sample is modeled as a homogeneous, one-layered material. Also within one sample small variations in material behavior can exist. The use of a strain map could allow to distinguish different homogeneous regions within a sample. However, only the resultant of the traction forces are available, whereas the amount of unknown parameters would increase. A numeric study should investigate whether and under which conditions it is possible to estimate parameter sets corresponding to different regions.

Note that in the current study we optimize traction forces, while in the past we optimized Cauchy stresses [**?**]. To calculate Cauchy stresses from the measured traction forces, you need to know the full deformation gradient and all nine traction force components. Since often not all force components can be measured, the assumption had to be made that the transversal forces and/or shear deformation were negligible. When optimizing traction forces, this assumption is no longer required.

In this study the GOH model [**?**] was chosen as the sample material. This material model is widely used in the community and is implemented in FE software packages. The results of this study are qualitative and a similar analysis can be made for a different material model.

Still, as all material models, the chosen model with two fiber families with a certain dispersion is only an approximation of the reality. Moreover, in reality the sample material is inhomogeneous. Investigating the influence of these assumptions should be the subject of future research.

5. Conclusion

The aim of this study was to obtain a better understanding of the implications of sample misalignment or an unknown sample orientation in planar biaxial testing using rakes. A series of finite element simulations were made, in which realistic PBR tests were simulated, after which the resulting quality of the parameter fitting procedure was evaluated. Several combinations of varia-

tions to the material and the test method were evaluated. These variations were related to

- the material model, two different sets of GOH parameters were used,
- the degree of sample rotation, i.e. $0°, 8°, 20°$ and $45°$,
- the assumption whether or not the sample orientation was assumed to be known,
- the use of a classical fitting procedure or a procedure that accounts for the inhomogeneous boundary conditions, and finally,
- whether or not a rail shear test was added to the planar biaxial test data.

For all test variations a difference between experimental and ground truth model traction forces is present, caused by the boundary conditions of the experimental set-up and assumptions made in the data processing. Therefore, in all cases, the importance of compensating for this difference, for example by using the BCC parameter fitting procedure, is evident.

For a perfectly aligned sample, the parameters of the GOH model can be found to a reasonable accuracy using a PBR test and the BCC parameter fitting procedure. For a slightly misaligned sample, using the BCC method will still allow you to find acceptable material parameters. However, after a certain threshold of misalignment, reliable parameters can no longer be found, despite the fact that the ground truth model traction forces can be accurately predicted with the resulting material parameters. The level of this threshold seems to be material dependent, which is why it is always important to carefully track the sample orientation during harvesting and preparation and minimize the misalignment.

A sample with fully unknown sample orientation, increases the number of parameters, or, in other words, uses a SEDF with an extra invariant. Material parameters could therefore theoretically be obtained by increasing the degrees of freedom along which test data is obtained, e.g. by adding a RS test. However,

in practice in the situation and the material model studied here, the inhomogeneous boundary conditions of the test set-ups render it impossible to obtain the correct parameters, even when using the BCC method. Unless more test data could be added to the fitting procedure, we therefore advise against attempts to fit the material properties of transversely isotropic samples for which the orientation is unknown.

6. Acknowledgements

The authors would like to thank Joris Gillis for his help with the implementation of CasADi and Optistack in our parameter fitting code. This work was supported by a pre- and post-doctoral fellowship of the Research foundation Flanders (FWO) (1S35316N and PDO-012) and a C2 project of internal KU Leuven funding (C24/16/026).

Appendix

Tables **??**, **??** and **??** show the material parameters fitting results and the quality measures of the different cases: 5-PBR, 6-PBR and 6-PBR+RS, respectively. In 5-PBR the sample orientation is assumed to be known and the sample is tested on a PBR. In 6-PBR and 6-PBR+RS the sample orientation is unknown and the sample is tested on a PBR and using a combination of a PBR and a RS test, respectively.

References

Table 3: Parameter fitting results of the Classic (C) and BCC procedure (BCC) of a sample of which the orientation is assumed to be known (5-PBR). One sample is tested in a PBR, hence in Equations **??** and **??** the number of samples s is 1 and the objective components $n = 11, 22$. For a correct sample orientation (MM1-0 & MM2-0), the parameter fitting results approximate the ground truth (GT) better with increasing the number of BCC iterations: decreasing NRMSE_{GT} . When a mistake is made in the sample orientation, this is reflected in the parameter fitting results.

Sample	Fitting	C_{10} [MPa]	k_1 [MPa]	k_2 [-]	κ [-]	α_1 [RAD]	α_2^* [RAD]	NRMSE_O [-]	MPE_{GT} [%]	NRMSE_{GT} [-]
MM1-0	GT	0.0770	0.0078	18.5600	0.2060	0.4800	2.6616			
	C	0.0630	0.0180	24.2441	0.2750	0.0002	3.1414	0.0982	11.04	0.1791
	BCC1	0.0781	0.0081	17.1337	0.1814	0.5274	2.6142	0.1093	1.22	0.1201
	BCC2	0.0754	0.0046	14.1103	0.1479	0.5533	2.5883	0.1376	3.78	0.0193
MM2-0	GT	0.0872	0.0063	3.3500	0.0000	0.2601	2.8815			
	C	0.0714	0.0109	4.8773	0.1217	0.0001	3.1415	0.1309	8.60	0.2062
	BCC1	0.0881	0.0080	3.6559	0.0128	0.2854	2.8562	0.0749	1.63	0.0467
	BCC2	0.0864	0.0067	3.6374	0.0176	0.2525	2.8891	0.0977	0.69	0.0093
MM1-8	GT	0.0770	0.0078	18.5600	0.2060	0.6196	2.8013			
	C	0.0630	0.0172	24.1895	0.2735	0.0002	3.1414	0.1024	10.46	0.1786
	BCC1	0.0779	0.0118	21.5030	0.2248	0.4531	2.6885	0.1708	3.61	0.1121
	BCC2	0.0760	0.0078	18.8919	0.2057	0.4847	2.6569	0.1643	1.01	0.0212
MM2-8	GT	0.0872	0.0063	3.3500	0.0000	0.3997	3.0212			
	C	0.0715	0.0105	4.7589	0.1209	0.0001	3.1415	0.1396	8.09	0.2074
	BCC1	0.0883	0.0111	4.8474	0.0917	0.1307	3.0109	0.1097	6.63	0.0391
	BCC2	0.0869	0.0070	3.5402	0.0031	0.3026	2.8390	0.1816	1.59	0.0249
MM1-20	GT	0.0770	0.0078	18.5600	0.2060	0.8290	3.0107			
	C	0.0630	0.0170	22.9730	0.2711	0.0001	3.1415	0.1674	9.86	0.1862
	BCC1	0.0788	0.0185	26.7723	0.2680	0.0001	3.1415	0.1848	10.61	0.0892
	BCC2	0.0787	0.0172	27.9222	0.2681	0.0001	3.1415	0.1935	10.25	0.1039
MM2-20	GT	0.0872	0.0063	3.3500	0.0000	0.0890	0.6091			
	C	0.0721	0.0107	4.5316	0.1426	0.0001	3.1415	0.1546	11.22	0.2037
	BCC1	0.0888	0.0120	4.8721	0.1273	0.0002	3.1414	0.2938	11.68	0.0217
	BCC2	0.0888	0.0112	5.1276	0.1259	0.0001	3.1415	0.2986	11.51	0.0217
MM1-45	GT	0.0770	0.0078	18.5600	0.2060	0.3054	1.2654			
	C	0.0625	0.0461	30.5825	0.3333	1.5708	1.5708	0.3215	35.83	0.2060
	BCC1	0.0787	0.0470	34.4307	0.3317	0.0005	3.1411	0.4226	28.37	0.0439
	BCC2	0.0788	0.0440	35.5418	0.3318	0.0005	3.1411	0.4236	27.30	0.0424
MM2-45	GT	0.0872	0.0063	3.3500	0.0000	0.5253	1.0455			
	C	0.0723	0.0634	1.8056	0.3333	1.5708	1.5708	0.1172	41.74	0.2010
	BCC1	0.0894	0.0801	0.0010	0.3167	0.7670	2.3746	0.2500	49.29	0.0329
	BCC2	0.0884	0.1178	0.0010	0.3146	0.7742	2.3674	0.3383	69.22	0.0667

* not a fitting parameter

Table 4: Parameter fitting results of the Classic (C) and BCC procedure (BCC) of a sample tested in a PBR of which the orientation is unknown (6-PBR). One sample is tested in a PBR, hence in Equations **??** and **??** the number of samples s is 1 and the objective components $n = 11, 22$. In some cases a good approximation of the ground truth parameters is found.

Sample	Fitting	C_{10} [MPa]	k_1 [MPa]	k_2 [-]	κ [-]	α_1 [RAD]	α_2 [RAD]	NRMSE$_O$ [-]	MPE$_{GT}$ [%]	NRMSE$_{GT}$ [-]
MM1-0	GT	0.0770	0.0078	18.5600	0.2060	0.4800	2.6616			
	C	0.0629	0.0143	21.7712	0.2561	0.0042	2.6490	0.0983	6.75	0.1800
	BCC1	0.0776	0.0083	17.7754	0.1910	0.5158	2.6346	0.1082	0.75	0.0855
	BCC2	0.0758	0.0037	12.6416	0.1203	0.6271	2.6179	0.1313	4.44	0.0119
MM2-0	GT	0.0872	0.0063	3.3500	0.0000	0.2601	2.8815			
	C	0.0700	0.0073	2.9354	0.0000	2.4972	3.1416	0.1034	4.48	0.2065
	BCC1	0.0855	0.0077	3.1652	0.0000	0.1813	2.7709	0.1069	1.77	0.0140
	BCC2	0.0867	0.0065	3.3362	0.0000	0.2402	2.8528	0.0804	0.36	0.0041
MM1-8	GT	0.0770	0.0078	18.5600	0.2060	0.6196	2.8013			
	C	0.0630	0.0089	17.4254	0.2159	2.4968	2.8638	0.0964	5.53	0.1787
	BCC1	0.0777	0.0132	26.2256	0.2467	0.3226	2.6967	0.1762	5.08	0.1599
	BCC2	0.0764	0.0069	18.2470	0.1931	0.5715	2.6943	0.1620	0.88	0.0382
MM2-8	GT	0.0872	0.0063	3.3500	0.0000	0.3997	3.0212			
	C	0.0696	0.0081	2.8751	0.0035	0.0000	0.7208	0.0976	6.65	0.2066
	BCC1	0.0854	0.0071	3.0224	0.0000	0.2112	2.8513	0.1160	2.15	0.0164
	BCC2	0.0872	0.0061	3.3629	0.0000	2.8039	2.9784	0.0977	4.21	0.0118
MM1-20	GT	0.0770	0.0078	18.5600	0.2060	0.8290	3.0107			
	C	0.0628	0.0025	8.9511	0.0600	0.8808	2.6757	0.0862	6.29	0.1885
	BCC1	0.0751	0.0048	15.9042	0.1789	0.7921	2.9895	0.1519	2.04	0.0688
	BCC2	0.0772	0.0019	9.5215	0.0495	0.4312	2.4275	0.1389	7.44	0.0176
MM2-20	GT	0.0872	0.0063	3.3500	0.0000	0.0890	0.6091			
	C	0.0693	0.0090	2.1873	0.0000	0.8548	2.9811	0.0796	11.63	0.2027
	BCC1	0.0833	0.0080	2.5276	0.0000	0.0420	0.5820	0.3046	3.15	0.0471
	BCC2	0.0856	0.0077	3.0654	0.0000	0.1316	0.6433	0.2481	2.39	0.0099
MM1-45	GT	0.0770	0.0078	18.5600	0.2060	0.3054	1.2654			
	C	0.0620	0.0041	9.3283	0.0942	0.4908	1.0796	0.0465	6.84	0.2027
	BCC1	0.0779	0.0050	19.9315	0.1755	0.4061	1.1457	0.2209	2.82	0.1826
	BCC2	0.0768	0.0027	15.7534	0.1191	0.4748	1.0829	0.2480	5.36	0.1491
MM2-45	GT	0.0872	0.0063	3.3500	0.0000	0.5253	1.0455			
	C	0.0673	0.0123	0.4477	0.0000	2.0783	2.6328	0.0722	13.90	0.2011
	BCC1	0.0884	0.0404	0.6978	0.2157	0.0000	1.3525	0.1440	21.47	0.0400
	BCC2	0.0764	0.0308	0.0010	0.0000	0.4956	2.0730	0.2260	16.81	0.0297

Table 5: Parameter fitting results of the Classic (C) and BCC procedure (BCC) of a sample of which the orientation is unknown tested using a PBR and a RS (6-PBR+RS). Two samples are tested, hence in Equations **??** and **??** the number of samples s is 2 and the objective components are $n = 11, 22$ for the sample tested in a PBR test and $n = 12$ for the sample tested in a RS test.

Sample	Fitting	C_{10} [MPa]	k_1 [MPa]	k_2 [-]	κ [-]	α_1 [RAD]	α_2 [RAD]	NRMSE$_O$ [-]	MPE$_{GT}$ [%]	NRMSE$_{GT}$ [-]
MM1-0	GT	0.0770	0.0078	18.5600	0.2060	0.4800	2.6616			
	C	0.0611	0.0201	19.2991	0.2548	0.3896	2.7519	0.2044	6.34	0.1837
	BCC1	0.0777	0.0078	17.2577	0.1963	0.4987	2.6429	0.1202	0.48	0.0164
	BCC2	0.0777	0.0063	17.4758	0.1905	0.5025	2.6391	0.1380	1.08	0.0122
MM2-0	GT	0.0872	0.0063	3.3500	0.0000	0.2601	2.8815			
	C	0.0697	0.0169	4.7470	0.1475	0.0001	3.1416	0.2268	9.83	0.2071
	BCC1	0.0858	0.0095	3.0001	0.0000	0.3804	2.7608	0.2604	3.15	0.0302
	BCC2	0.0849	0.0097	2.8523	0.0000	0.3992	2.7420	0.3331	3.61	0.0316
MM1-8	GT	0.0770	0.0078	18.5600	0.2060	0.6196	2.8013			
	C	0.0614	0.0170	19.3124	0.2483	0.5898	2.9735	0.1780	4.83	0.1847
	BCC1	0.0776	0.0077	17.0959	0.1943	0.5787	2.7123	0.1080	0.71	0.0181
	BCC2	0.0776	0.0062	17.1344	0.1876	0.5777	2.7045	0.1232	1.34	0.0138
MM2-8	GT	0.0872	0.0063	3.3500	0.0000	0.3997	3.0212			
	C	0.0696	0.0158	4.4215	0.1354	0.2515	3.1416	0.1784	7.15	0.1959
	BCC1	0.0858	0.0094	2.9115	0.0000	0.4490	2.8017	0.1279	2.32	0.0303
	BCC2	0.0883	0.0052	3.6301	0.0000	0.4733	3.1237	0.1290	1.36	0.0306
MM1-20	GT	0.0770	0.0078	18.5600	0.2060	0.8290	3.0107			
	C	0.0615	0.0119	17.1710	0.2231	0.8175	3.1294	0.1680	2.61	0.1878
	BCC1	0.0774	0.0074	15.8951	0.1841	0.6948	2.7639	0.2091	1.53	0.0325
	BCC2	0.0772	0.0060	15.2941	0.1734	0.6830	2.7504	0.2193	2.31	0.0378
MM2-20	GT	0.0872	0.0063	3.3500	0.0000	0.0890	0.6091			
	C	0.0694	0.0152	3.6422	0.1210	0.0192	0.5709	0.2425	7.42	0.2087
	BCC1	0.0858	0.0093	2.4240	0.0000	0.6184	2.8069	0.2815	15.40	0.0285
	BCC2	0.0884	0.0050	3.2600	0.0000	0.6281	3.1366	0.3441	3.71	0.0206
MM1-45	GT	0.0770	0.0078	18.5600	0.2060	0.3054	1.2654			
	C	0.0620	0.0076	15.3639	0.1983	0.3157	1.2492	0.2276	1.32	0.2116
	BCC1	0.0776	0.0070	17.5273	0.1976	1.2184	2.7254	0.2534	7.24	0.0232
	BCC2	0.0774	0.0066	17.0763	0.1945	1.2160	2.7177	0.2974	7.56	0.0192
MM2-45	GT	0.0872	0.0063	3.3500	0.0000	0.5253	1.0455			
	C	0.0701	0.0078	3.6895	0.0428	0.4876	1.0768	0.2068	1.89	0.2135
	BCC1	0.0900	0.0058	5.1652	0.0682	0.6132	0.9723	0.3006	2.66	0.0205
	BCC2	0.0901	0.0045	4.8442	0.0541	0.7057	0.8803	0.2987	3.67	0.0207

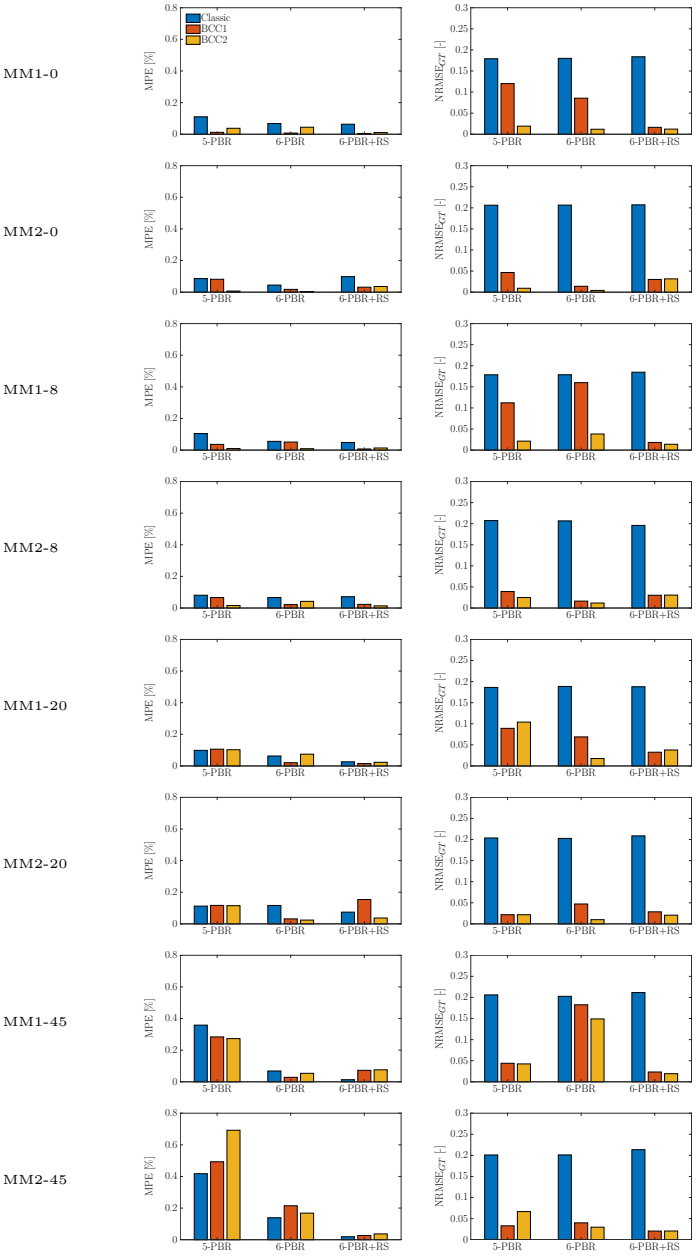

Figure 14: Measures to asses how well the fitting results approximate the ground truth for all samples for the various cases. The BCC parameter fitting results in a better approximation of the ground truth.

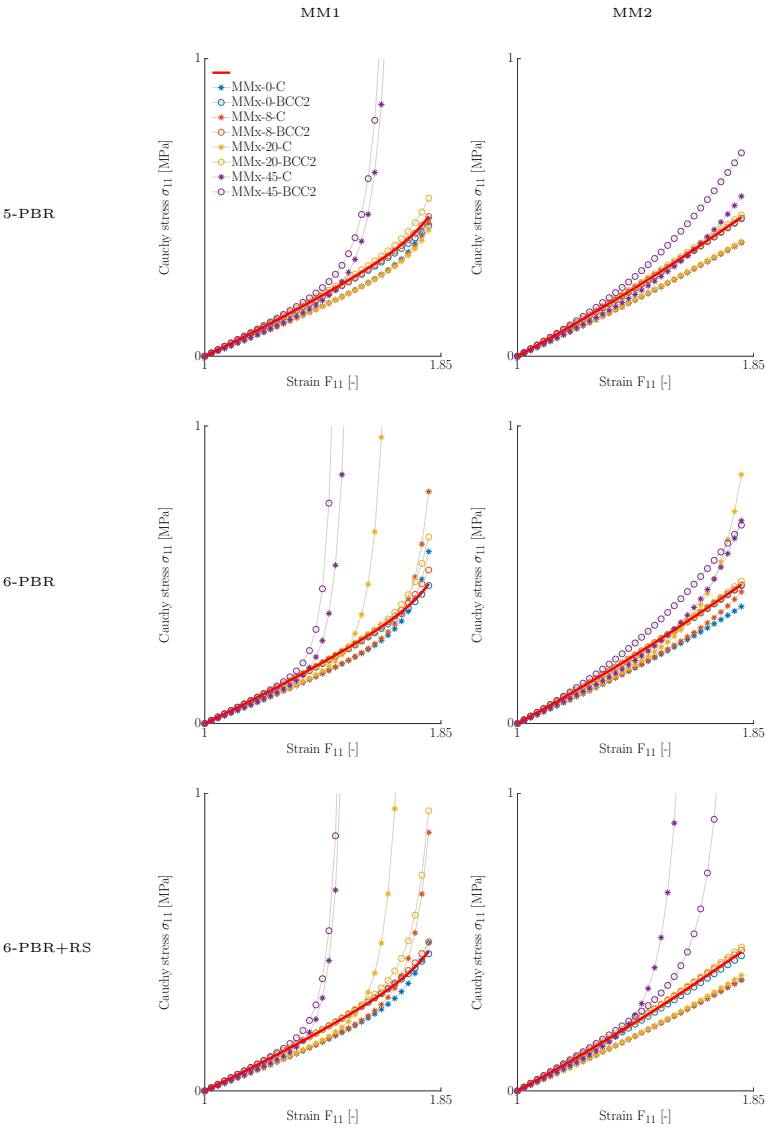

Figure 15: Resulting stress-strain curves when the fitted material parameters are extrapolated to a uniaxial test. The stress strain-curve calculated with the ground truth material parameters is the full blue line. The parameters obtained via BCC parameter fitting (∘) perform better than those obtained through Classic parameter fitting (⋆).